Heat generation in plasmonic nanostructures: Influence of morphology

G. Baffou,[1,a] R. Quidant,[1,2] and C. Girard[3]
[1]*ICFO-Institut de Ciencies Fotoniques, Castelldefels, Barcelona 08860, Spain*
[2]*ICREA-Institució Catalana de Recerca i Estudis Avançats, Barcelona 08010, Spain*
[3]*CEMES, CNRS, Université Paul Sabatier, 29 rue J. Marvig, F-31005 Toulouse, France*

(Received 2 March 2009; accepted 20 March 2009; published online 16 April 2009)

Using the Green's dyadic method, we investigated numerically the heat generation in gold nanoparticles when illuminated at their plasmonic resonance. Two kinds of structures are discussed—colloidal-like nanoparticles and lithographic planar nanostructures—putting special emphasis on the influence of the object's morphology at a constant metal volume. The mechanism of heating is explained and discussed by mapping the heating power density inside the structures. This work aims at giving an intuitive and original understanding of the relative heating efficiency of a wide set of morphologies and could stand for a basis recipe to design optimized plasmonic nanoheaters. © *2009 American Institute of Physics*. [DOI: 10.1063/1.3116645]

Heat generation in plasmonic nanoparticles induced by light absorption has long been considered only as a side effect, which had to be minimized, e.g., for imaging techniques in biology or molecular fluorescence enhancement. Since recently, it has been realized and demonstrated that metal nanoparticles can play the role of efficient nanosources of heat, which opens up a new emerging set of applications in nanotechnology, merging the fields of nanothermodynamics[1,2] and nano-optics,[3] and giving rise to a new promising field that could be named *thermoplasmonics*. The number of potential applications of thermoplasmonics is becoming more and more important in areas of nanotechnology such as photothermal cancer therapy,[4–8] drug delivery, materials science,[9–11] nanofluidics,[9,12,13] and phononics.[14–16] While lots of efforts have been done to optimize the morphology of a plasmonic nanostructure when acting as light scatterers, enhancers, or nanoantennas, morphology optimization for local heating remains quite unexplored theoretically.

In this paper, we use the Green' dyadic method (GDM)[17,18] to investigate numerically and quantitatively the heating efficiency of two kinds of homogeneous gold nanostructures used in plasmonic heating applications: colloidal nanoparticles (spheres and nanorods) in water and planar nanostructures on glass. The first set of structures is related to applications in aqueous medium such as in medicine and biology,[4–8] and the second set is more related to lithographic structures lying onto a glass sample surrounded by a fluid medium.[9–11] All the structures investigated in this paper have been assigned the same volume in order to focus specifically on morphology effects. The GDM allows for mapping the spatial distribution of the heat power density inside the nanoparticles, which enables us to understand and explain in detail the origin of heating as a function of the morphology and the wavelength.

When a metal nanoparticle is illuminated, part of the intercepted light is scattered in the surroundings, while the other part gets absorbed and ultimately dissipated into heat.[19] The efficiency of each of these processes can be characterized by σ_{sca} and σ_{abs}, the elastic scattering and the absorption cross sections, respectively. The sum of these two processes leads to light attenuation characterized by the extinction cross section σ_{ext},

$$\sigma_{ext} = \sigma_{sca} + \sigma_{abs}. \tag{1}$$

Depending on the size and the shape of the nanoparticle, the balance between scattering and absorption can substantially vary.[20–26] For instance, while small gold spheres (<10 nm in diameter) mainly act as invisible nanosources of heat,[27,28] scattering processes dominate for diameters larger than ~ 50 nm.[20] In the scope of this paper, we will focus on the absorption processes and the subsequent heat generation. In order to discard the volume effect mentioned above and to focus on morphology effects, all the structures are assigned a common volume $v_0=(4\pi/3)r_c^3$, where the effective radius r_e is fixed at 25 nm. The general expression of the absorption cross section for a nanoparticle illuminated by a plane wave is (in mks units),

$$\sigma_{abs} = \frac{k}{\varepsilon_0 |\mathbf{E}_0|^2} \int_{NP} \mathrm{Im}(\varepsilon_\omega) |\mathbf{E}(\mathbf{r})|^2 d\mathbf{r}, \tag{2}$$

where $k=2\pi n/\lambda_0 = n\omega/c$ is the wave vector, n is the optical index of the surrounding medium, ε_ω is the permittivity of the nanoparticle material, $\mathbf{E}_0$ is the electric field amplitude of the incoming light considered as a plane wave, and $\mathbf{E}(\mathbf{r})$ is the total electric field amplitude. The integral is calculated over the nanoparticle volume. The power of heat generation $\mathcal{Q}$ inside the nanostructure is directly proportional to σ_{abs},

$$\mathcal{Q} = \sigma_{abs} I = \sigma_{abs} \frac{nc\varepsilon_0}{2} |\mathbf{E}_0|^2, \tag{3}$$

where $I=(nc\varepsilon_0/2)|\mathbf{E}_0|^2$ is the irradiance of the incoming light, and using Eq. (2) we obtain

$$\mathcal{Q} = \frac{n^2\omega}{2} \mathrm{Im}(\varepsilon_\omega) \int_{NP} |\mathbf{E}(\mathbf{r})|^2 d\mathbf{r} = \int_{NP} q(\mathbf{r}) d\mathbf{r}, \tag{4}$$

where $q(\mathbf{r})=(n^2\omega/2)\mathrm{Im}(\varepsilon_\omega)|\mathbf{E}(\mathbf{r})|^2$ is the volumetric power density of heat generation. The calculation of the absorption coefficient thus requires the knowledge on the electric field amplitude inside the nanoparticle. To calculate it, we used the GDM.[17,18] In our calculations, the structures are meshed with a number of cells varying from 2500 to 9000 depending on the geometry and the convergence requirements. The

[a]Electronic mail: guillaume.baffou@icfo.es.

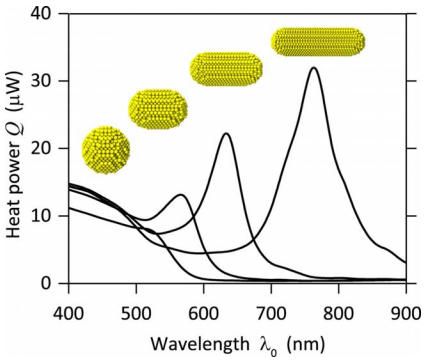

FIG. 1. (Color online) Calculated spectra of the heat generated in four different colloidal gold nanoparticles of the same volume.

meshing uses a hexagonal close-packed lattice.[18] This has the advantage over the usual cubic meshing to lead to a better space filling and is better suited for structures presenting threefold symmetries. In all the following calculations, we consider that the intensity of the incoming light is $I=1\ \mathrm{mW}/\mu\mathrm{m}^2=10^5\ \mathrm{W}/\mathrm{cm}^2$, according to the typical value found in literature.[2]

Figure 1 displays calculations of heating power spectra for gold nanoparticles illuminated by a plane wave in a homogeneous and isotropic surrounding medium characterized by its refractive index $n=1.33$. This configuration is intended to model situations where the colloidal nanoparticles are immersed in aqueous medium, like in biological applications. For instance, gold nanorods are foreseen to be ideal candidates for photothermal cancer therapy because their resonance of the heat generation can easily be tuned into the transparency spectral window of human tissue (λ_0 ranging from 700 to 900 nm). We investigated the heat generation of a sphere progressively deforming itself into a rodlike structure at a constant volume. The successive nanorod aspect ratios are 1:1 (sphere), 1.4:1, 2:1, and 3:1. Two major features arise from the calculations. First the localized surface plasmon (LSP) resonance markedly depends on the nanoparticle shape. A redshift is indeed expected for nanorods compared to spheres. Then, the redshift occurs along with a substantial increase in the heating efficiency: around 60% variation from the sphere to the 3:1 nanorod. The GDM can be efficiently employed to understand this feature. Figure 2 represents the meshed nanostructures with a color scale related to the heating power density $q(\mathbf{r})$. On the right side, cross cuts are performed in the meshing to reveal the heating power density of the inner parts of the structures. Interestingly, for a sphere excited at its LSP resonance, the heating generation arises mainly from the outer part of the particles facing the incoming light. Consequently, the major part of the nanoparticle remains inactive since it is deeply buried and does not contribute to heating. However, for elongated nanorods, the inner part of the particle gets closer to the outer part and no longer suffers from this shielding effect. The whole volume of the structure is thus more efficiently involved in the heating process, which mainly explains the pronounced increase in the heating efficiency. It should be underlined that the heat generation mainly arises from the center part of the nanorods because the extremities undergo charge accumulation and thus a weaker electric field inside the structure.

Note that the maps represented in Fig. 2 must not be assimilated to the temperature distribution inside the nanoparticles. Indeed, the temperature distribution $T(\mathbf{r})$ generated by the heating power density distribution $q(\mathbf{r})$ is governed by the Poisson equation,

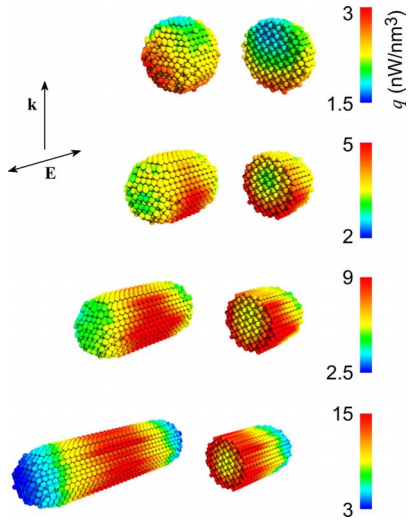

FIG. 2. (Color online) Three-dimensional (3D) mapping of the heat power density computed for the four nanoparticles of Fig. 1 at their respective plasmon resonance.

$$\kappa\nabla^2 T(\mathbf{r}) = -q(\mathbf{r}), \tag{5}$$

where κ (=318 W/m K) is the thermal conductivity of gold. A dimensional analysis of this equation permits one to estimate the expected temperature *spatial* variation δT throughout the structure,

$$\delta T \sim \frac{l^2}{\kappa}\frac{Q}{v_0}, \tag{6}$$

where l is the typical spatial dimension of the structure. Using this formula, we can expect temperature spatial variation in approximately 0.1 °C along the nanoparticle. This amounts to saying that the nanoparticle's temperature is quasiuniform even though the heat generation is clearly not. Such a small value comes from the very small spatial dimension of the system: at this scale, the thermal diffusion is so fast that, even though the heating power density undergoes strong spatial variations, the temperature diffuses quickly and remains almost uniform. The steady state temperature increase depends on how efficient the thermal diffusion through the surroundings is, which is characterized by its thermal conductivity κ_0 (=0.6 W/m K for water). The Poisson equation [Eq. (5)] is easy to solve analytically with spherical symmetry. Outside the nanoparticle, it simply gives

$$\hat{T}(\mathbf{r}) = \hat{T}_0\frac{r_e}{r}, \tag{7}$$

where the notation $\hat{T}(\mathbf{r})$ defines the temperature increase above the room temperature and $\hat{T}_0$ is the temperature increase inside the nanoparticle, considered as uniform. Then, $\hat{T}_0$ can be calculated by equaling the heat power Q to the integral of the energy current density $\mathbf{j}_{\mathrm{th}}=-\kappa_0\nabla T$ over the sphere boundary, which gives

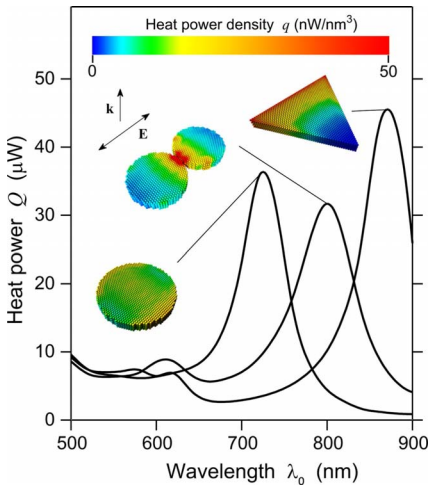

FIG. 3. (Color online) Calculated spectra of the heat generated in structures deposited on a planar glass surface immersed in water. The three insets represent the 3D heat power density computed at the main plasmon resonance of the particle.

$$\hat{T}_0 = \frac{1}{4\pi\kappa_0 r_e}\frac{\mathcal{Q}}{}. \tag{8}$$

For the gold sphere investigated above, we find that the temperature increase is $\hat{T}_0 = 13\ ^\circ\mathrm{C}$, which is of the order of magnitude of the values reported in literature.[2]

Figure 3 displays calculations of heating power spectra for planar gold nanoparticles lying onto a glass substrate and surrounded by water. This configuration is more related to lithographic nanostructures around which thermal effects, such as convection of the surrounding fluid, have been evoked but not well understood.[9] We study the heat generation of a disk, a dimer and a triangle keeping the gold volume (v_0) and height ($h_0 = 12$ nm) constant. Unlike the colloids case, while one can observe the expected redshift when deforming the disk into a dimer or a triangle, the heating efficiency does not undergo substantial variations. Beyond, all the planar geometries considered here feature greater heating efficiency than the nanorods discussed in Fig. 1, although the gold volume is the same. This high heating ability arises from the same effect that makes nanorods more efficient heaters than spheres; by using thin planar structures one can reduce the shielding effect mentioned above. It appears that the thinner the structure, the higher the heating efficiency. Moreover, in practice the noncrystallinity of lithographic structures should further increase the energy dissipation and favor heat generation making them fundamentally more efficient nanosources of heat compared to crystalline colloidal particles.

The insets in Fig. 3 represent the heating power density distributions for each geometry. The most efficient heating observed for the triangle seems to show that corners and sharp edges are favorable for heat generation. Conversely, the lower heating efficiency observed for the dimer reveals that the presence of a gap is not particularly beneficial. For a dimer, the enhanced electric field is located within the gap. In order to optimize the heat generation in a nanoparticle, the square electric field has to be optimized inside the structure [see Eq. (2)] and not outside, explaining why a dimer structure does not lead particularly to high heating efficiency.

In conclusion, the GDM appears to be a very efficient tool to investigate the mechanisms of heating effects and the heating efficiency of plasmonic nanoparticles. This method enabled us to quantify the heat generation in a wide set of nanoparticles and to map the internal distribution of the heating power density. To focus on geometry effects and get rid of size effects, all the structures have been assigned an identical volume. We have shown that while an increase in the electric field has to be optimized *outside* the structures for most applications in optics, one have to think of the opposite way for photothermal applications where the electric has to be optimized *inside* the nanoparticle. As a consequence, the presence of small gaps between adjacent particles do not provide any increase in heating efficiency. However, small, flat, elongated, or sharp nanoparticles appear to be much more efficient heaters than massive nanostructures. These effects come from the fact that the incoming electric field penetrate more easily inside the thin nanostructures making the whole amount of gold matter involved in heating. These results could be the basis of the design of new optimized nanostructures for photothermal applications using plasmonic nanoparticles.

This research has been funded by the Spanish Ministry of Sciences through Grant Nos. TEC2007-60186/MIC and CSD2007-046-NanoLight.es and by the fundació Cellex Barcelona.

[1] *Microscale an Nanoscale Heat Transfer*, edited by S. Volz (Springer, Berlin, 2007).
[2] A. O. Govorov and H. H. Richardson, Nanotoday **2**, 30 (2007).
[3] L. Novotny and B. Hecht, *Principles of Nano-Optics* (Cambridge University Press, Cambridge, 2006).
[4] A. M. Gobin, M. H. Lee, N. J. Halas, W. D. James, R. A. Drezek, and J. L. West, Nano Lett. **7**, 1929 (2007).
[5] D. Pissuwana, S. M. Valenzuelaa, and M. B. Cortie, Trends Biotechnol. **24**, 62 (2006).
[6] P. K. Jain, I. H. El-Sayed, and M. A. El-Sayed, Nanotoday **2**, 18 (2007).
[7] G. Han, P. Ghosh, M. De, and V. M. Rotello, NanoBio Technology **3**, 40 (2007).
[8] A. G. Skirtach, C. Dejugnat, D. Braun, A. S. Susha, A. L. Rogach, W. J. Parak, H. Möhwald, and G. B. Sukhorukov, Nano Lett. **5**, 1371 (2005).
[9] M. Righini, A. S. Zelenina, C. Girard, and R. Quidant, Nat. Phys. **3**, 477 (2007).
[10] V. Garces-Chavez, R. Quidant, P. J. Reece, G. Badenes, L. Torner, and K. Dholakia, Phys. Rev. B **73**, 085417 (2006).
[11] L. Cao, D. Barsic, A. Guichard, and M. Brongersma, Nano Lett. **7**, 3523 (2007).
[12] G. L. Liu, J. K. Yu Lu, and L. P. Lee, Nature Mater. **5**, 27 (2006).
[13] D. Ross, M. Gaitan, and L. E. Locascio, Anal. Chem. **73**, 4117 (2001).
[14] C. W. Chang, D. Okawa, A. Majumdar, and A. Zettl, Science **314**, 1121 (2006).
[15] L. Wang and B. Li, Phys. Rev. Lett. **101**, 267203 (2008).
[16] N. Yang, G. Zhang, and B. Li, Appl. Phys. Lett. **93**, 243111 (2008).
[17] O. J. F. Martin, C. Girard, and A. Dereux, Phys. Rev. Lett. **74**, 526 (1995).
[18] C. Girard, E. Dujardin, G. Baffou, and R. Quidant, New J. Phys. **10**, 105016 (2008).
[19] D. R. Bohren and C. F. abd Huffman, *Absorption and Scattering of Light by Small Particles* (Wiley, New York, 1983).
[20] P. K. Jain, K. S. Lee, I. H. El-Sayed, and M. A. El-Sayed, J. Phys. Chem. B **110**, 7238 (2006).
[21] N. Harris, M. J. Ford, and M. B. Cortie, J. Phys. Chem. B **110**, 10701 (2006).
[22] K. S. Lee and M. A. El-Sayed, J. Phys. Chem. B **109**, 20331 (2005).
[23] A. L. Gonzalez and C. Noguez, J. Comput. Theor. Nanosci. **4**, 231 (2006).
[24] S. Link and M. A. El-Sayed, Int. Rev. Phys. Chem. **19**, 409 (2000).
[25] K. L. Kelly, E. Coronado, L. L. Zhao, and G. C. Schatz, J. Phys. Chem. B **107**, 668 (2003).
[26] E. Hao, G. C. Schatz, and J. T. Hupp, J. Fluoresc. **14**, 331 (2004).
[27] D. Boyer, P. Tamarat, A. Maali, M. Lounis, and B. Orrit, Science **297**, 1160 (2002).
[28] S. Berciaud, D. Lasne, G. A. Blab, L. Cognet, and B. Lounis, Phys. Rev. B **73**, 045424 (2006).